Environ Geol
DOI 10.1007/s00254-007-0761-3

ORIGINAL ARTICLE

Evaluation of landfill disposal boundary by means of electrical resistivity imaging

Vladimir Frid · Gady Liskevich · Dmitriy Doudkinski · Nikolay Korostishevsky

Received: 7 December 2006 / Accepted: 10 April 2007
© Springer-Verlag 2007

Abstract This paper deals with an employment of electrical resistivity imaging (ERI) for survey of leachate content on the waste disposal site in Northern Israel. The research consisted of conducting ten ERI lines and drilling investigation wells. Data simulation used a 2D EarthImager inversion program. Analysis of 2D ERI interpretation results shows that determination of the boundary between the landfill body bottom intensively saturated with leachates and underlying layers of highly water saturated fat non-consolidated clays presents a challenge. However, statistical analysis of ERI data indicates that standard deviation and confidence interval of a set of resistivity data measured in the landfill body are significantly larger than those in underlying clays. Moreover, maximum changes of these parameters are found on the boundary between landfill body and underlying soil, thus reflecting natural differences in scattering of resistivity data measured in these two objects.

Keywords Waste landfill · Electrical imaging survey · Electrical resistivity tomography

Introduction

Monitoring of water contamination induced by municipal landfills usually includes leachate and water sampling from drilled well network, and chemical analysis of samples taken from and around the landfill disposal under investigation (Martinho and Almeida 2006; Abu-Zeid et al. 2004). This investigation method provides a discontinuous subsurface picture and can be a very tedious and expensive procedure (Zume et al. 2006). That is the reason why an interest in applying nondestructive and noninvasive surface geophysical methods has increased. Electrical resistivity imaging (ERI) is a modified direct current method (Khesin et al. 1996) and is based on the dependence of electrical resistivity of different materials on the content of moisture and high conductive elements, porosity, temperature, etc. (Aristodemou and Thomas-Betts 2000; Gawande et al. 2003; Guerin et al. 2004).

Electrical resistivity imaging has been enjoying wide application (Sharma 1997; Takahashi 2004; Khesin 2005; Takahashi et al. 2006) since the end of the twentieth century when rapid progress of geophysical equipment based on computer technique allowed the use of 2D/3D observation schemes (Loke and Barker 1995, 1996a, b; Dahlin and Loke 1998; Storz et al. 2000; Dahlin 2001; Hunt et al. 2001; Dahlin and Zhou 2002, 2004; Wu et al. 2003; Cardarelli and Fischanger 2006). It has been frequently employed for material characterization in various geo-engineering applications: aquifer investigations (Chandra et al. 2006; Froese et al. 2005; Loke 2000; Nassir et al. 2000; Storz et al. 2000; Bowling et al. 2005; Porsani et al. 2005; Hamzah et al. 2006; Sherif et al. 2006), archeological surveys (Cardarelli and Bernabini 1997; Vafidis et al. 2005; DeDominico et al. 2006; Dogan and Papamarinopoulos 2006), land- and rock slide characterizations (Grandjean et al. 2006; Loke 2000; Drahor et al. 2006; Godio et al. 2006), karst and fracturing mapping (Leucci 2006; Gibert et al. 2006; Recelli-Snyder et al. 1997; Loke 2000), fault imaging (Rizzo et al. 2004; Nguyen et al. 2005), and agricultural study (Loke 2000; Pannisod et al. 2001; Rey et al. 2006).

V. Frid (✉) · G. Liskevich · D. Doudkinski · N. Korostishevsky
Geotechnical Department,
Isotop, POB 2, Gedera 70700, Israel
e-mail: vfrid@bgu.ac.il; vladifrid@gmail.com

Application of ERI method to waste landfill characterization is very popular because electrical resistivity of waste in landfill disposal varies considerably with time during waste decomposition and leachate formation (Cardarelli and Bernabini 1997; Aristodemou and Thomas-Betts 2000; Bernstone et al. 2000; Gawande et al. 2003; Abu-Zeid et al. 2004; Guerin et al. 2004; Batayneh and Barjous 2004; Depountis et al. 2005; Martinho and Almeida 2006; Zume et al. 2006).

Study area and aim

Our study area is known as ''Har HaAshpaa'' (''Waste Hill'' in English translation), it was started by British Army in 1944. It is located in the coastline part of Haifa city (with a population of about 267,800 as of May 2006) in Northern Israel about 100 km away from the Tel Aviv downtown (Fig. 1). During 1944–1949, the site was uncontrollably and exclusively filled by the British Army waste. All topographic records of the site prior to the disposal are unknown because all documents of British Army were lost. Haifa municipality used the site for domestic waste disposal from 1949 till the end of 1999. In the last operation year, waste input rate reached about 300–400 ton of domestic waste per day (Gurion and Novik 2003).

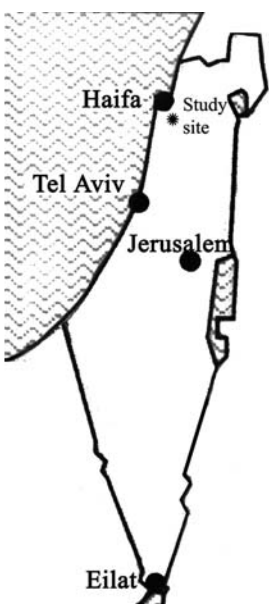

Fig. 1 Scheme of the study site location

The soils overlapped by the landfill body are mainly clays of recent or pre-recent (Holocene) age. Three lithological facies are derived: (1) brownish soft fat clays, (2) grey very soft fat clays, and (3) rarely soft clayey sand. The last named facia occurs in the upper part of the soil column and is frequently interbedded with clay varieties. Total thickness of both clay varieties is about 12 m. The mechanism for the soil formation is sedimentation under shallow marine (lagoon) conditions without being overburdened by younger sediments, which causes low-density soil (900–1,000 kg/m^3), its high water saturation (45–60%) and low consolidation (typical overconsalidation ratio of about 0.2). Being not absolutely isolated from the open sea, soils on the site under investigation exhibit moderately high sand content in the clays and hence low values of Atterberg limits and free swelling.

Electrical resistivity of clays is known to be in the range 3–150 ohm m (Table 1), while electrical resistivity of water (from sea to salted or brackish water) changes between 0.1 and 5 ohm m (Bernstone et al. 2000; Guerin et al. 2004). As is known, electrical resistivity of two component medium ρ depends on values of electrical resistivities of both components $\rho = f(\rho_s, \rho_l)$, where ρ_s and ρ_l are electrical resistivities of solid and liquid components of liquid saturated medium, respectively. Therefore, electrical resistivity of water-saturated clay (1.5–30 ohm m) is very similar to that of leachate (0.9–5 ohm m, Table 1), with the result that determination of a boundary between leachate-saturated waste and water-saturated clay is difficult.

This research was motivated by the necessity to estimate the degree of impact of waste landfill body on regional environment where the top challenge was an accurate defining of the boundary between waste disposal and underlying soil.

Equipment and method

Our multidisciplinary research consisted of conducting ten ERI lines. The programmable Sting R1–Swift system

Table 1 Electrical resistivity for different materials

Soil/material	Resistivity, ohm m	References
Clay	3–150	Guerin et al. (2004); Hack (2000); Kneisel (2006)
Salt water saturated clay	1.5–2	Abu-Zeid and Santarato (2004)
Leachate	0.9–5	Guerin et al. (2004); Zume et al. (2006)
Domestic garbage	12–30	Hack (2000)
Scrap metal	1–12	Hack (2000)

manufactured by the Advanced Geoscience, Inc. (Austin, TX, USA) was used for data collection in our ERI investigation. It comprised Sting R1 resistivity meter, the Swift automatic multielectrode switching box, cables, and special electrode assemblages including stainless steel switches attached to grounded stainless steel rods. Thirty of such smart electrodes arranged in Schlumberger configuration were utilized along each ERI line. Ten ERI lines were conducted in the area under investigation, their length varied in the range from 150 to 420 m, while the inter-electrode spacing varied between 5 and 6 m. Lines longer than 150–180 m were carried out in the roll-along manner.

The AGI Earth Imager 2D software (version 2.1.2) was employed for smooth apparent resistivity inversion to produce 2D model of the estimated true subsurface resistivity. This procedure uses Gauss–Newton least squares method (Loke and Dahlin 2002) based on the initiation of a finite-element model of the underground surface. The finite element model of electrical resistivities are automatically modified through an iterative process, so that the model response converges towards the measured data (Loke and Barker 1996b). The mean residual value (RMS) is a measure of fit between measured apparent resistivities and the apparent resistivities of the model response from the inverted resistivity (Bernstone et al. 2000). Stabilizing and damping factors, needed to balance data misfit and to speed up the convergence inversion process in early stages, were considered to be 10. Cholesky decomposition forward equation solver and mixed boundary conditions were employed to produce proper inversion of ERI data by the AGI's recommendations and our own experience.

Results of EIS investigation and their discussion

Figure 2 shows the examples of vertical inverted resistivity section and the cross plot of measured versus predicted apparent resistivity. As seen, RMS error in Fig. 2b is about 3%, implying a good fit between them and hence reasonable accuracy of inverted resistivity section. Note that RMS of all ten conducted lines varied from 2.5 to 5% suggesting fair accuracy of inverted sections.

The scatter of the electrical resistivities of all data sets measured is very wide, from 0.1 up to 10,000 ohm m. Nevertheless, 95% of the whole data set offers electrical resistivity less than 450 ohm m and electrical resistivities corresponding to leachates (0.9–5 ohm m, Guerin et al. 2004; Zume et al. 2006) or water saturated clays are between 3 and 30 ohm m depending on measurement depth. Analysis of Fig. 2a shows that vertical section can be roughly divided into about two equal parts. The upper part of the vertical section comprises materials characterized by electrical resistivity between 5 and 30 ohm m (see color scale at the right side of Fig. 2a). This range of electrical resistivity corresponds to the existence of domestic garbage (Table 1) and clays on the waste site. As we noted above, the waste landfill was mainly used for domestic garbage disposal from 1949 to 1999, and hence this observation seemed self-consistent to us. The lower part of the vertical section consists of materials whose electrical resistivity is in the range of 0.9–5 ohm m implying the existence of leachate or salt water saturated clay there (Table 1). Analysis of Fig. 2a demonstrates that the boundary between the bottom part of the landfill body and underlying water-saturated fat clays cannot be found accurately due to their similar resistivities.

Figure 3 shows changes of volume and area of ''wet zones'' (where electrical resistivity was measured to be in the range of 0.9–5 ohm m) at different depths of the waste landfill body. As can be seen, the volume and the area of ''wet zones'' increase with the depth of the landfill body below 20 m above the sea level and tend to decrease below the depth of 0 to –2 m.

Statistical analysis of the whole data set of electrical resistivity values measured on the site showed that standard deviation alteration (and those of confidence interval at the 95% level) with the depth of the waste landfill body can be divided into three main intervals: upper 25–31 m depth, intermediate –2 to 25 m depth, and lower –2 to –21 m depth. Note that confidence level was calculated as follows $\pm 1.96\sigma/\sqrt{n}$, where ±1.96 is the area under the standard normal curve corresponding to confidence level 95%, σ is the standard deviation, n is the sample size while only positive values of confidence interval were taken into consideration.

Standard deviation values (and confidence interval values) are relatively low in the lower interval. Intermediate interval shows an increase in their values. Standard deviation (and confidence interval) peaks at the depth of –1 to –2 m, followed by a sharp decrease (Fig. 4a). To quantify standard deviation and confidence level changes, we calculated two new parameters as follows and termed them as standard deviation rate (SDR) and confidence level rate (CLR):

$\mathrm{SDR} = (\mathrm{SD}_i - \mathrm{SD}_{i+1})/(\mathrm{H}_i - \mathrm{H}_{i+1})$ and $\mathrm{CLR} = (\mathrm{CL}_i - \mathrm{CL}_{i+1})/(\mathrm{H}_i - \mathrm{H}_{i+1})$, where $\mathrm{SD}_i(\mathrm{CL}_i)$ and $\mathrm{SD}_{i+1}(\mathrm{CL}_{i+1})$ are the standard deviation (confidence level) of two consequent layers of landfill disposal. H_i and H_{i+1} are the depths of two consequent layers of landfill disposal ($\mathrm{H}_i > \mathrm{H}_{i+1}$). Figure 4b shows that maximum values of SDR and CLR are at the depth of –2.5 m implying probably maximum differences in the data spread on the boundary between artificially (landfill disposal) and naturally (underlying soil) formed objects. Two investigation wells drilled through the entire waste body down to the bottom boundary of the waste landfill indeed confirmed the assumption: the

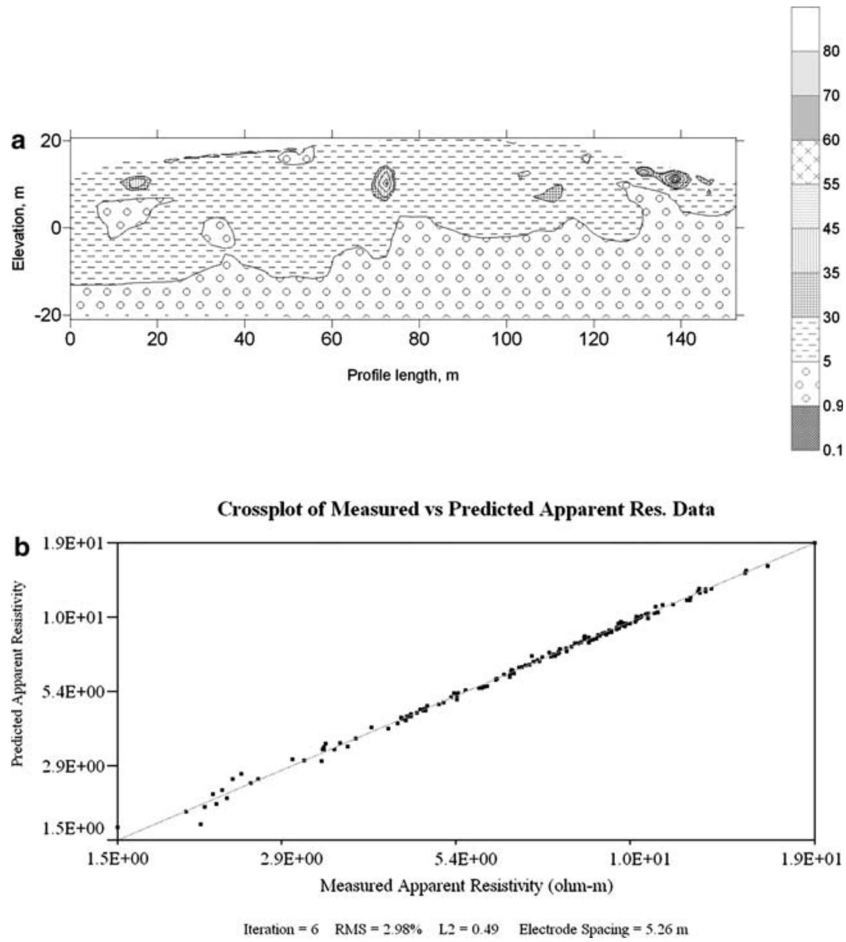

Fig. 2 **a** An example of inverted resistivity section. **b** Cross plot of measured versus predicted apparent resistivity. See explanation in the text

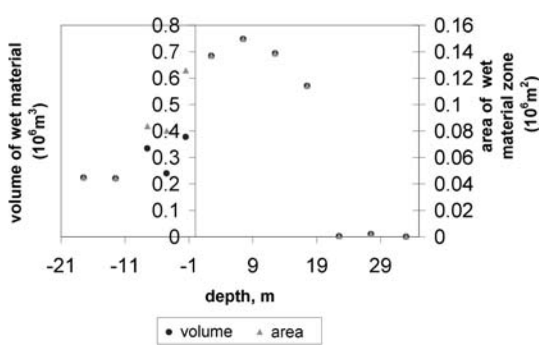

Fig. 3 Changes of volume and area of the ''wet zone'' versus depth of the waste body. ''Wet zone'' was defined as the zone with the resistivity between 0.9 and 5 ohm m

boundary between the waste disposal and underlying fat clays was found at the depth of –2 to –3 m below the sea level.

A self-consistency of our results seems to be understandable because dissimilarity in the spreads of two data sets originates from the difference in their genesis. The spread of electrical resistivity measured in the waste disposal, which is a heterogeneous object of artificial origin, must be much larger than that measured in naturally formed object such as the soil underlying the waste body. Therefore, the transition from the waste disposal to the underlying soil is marked by a ''jump'' in the spread of electrical resistivity measured.

Our results show that total volume of ''wet zones'' (Fig. 3) in and under the waste disposal is estimated to be of about 3.5 million m^3. Our method enables us to distinguish between ''wet zones'' in and under the waste disposal, the total volumes of which were estimated to about 2.5 million m^3 and 1 million m^3, respectively (Fig. 3). Analysis of Fig. 4 shows that oscillations of standard deviation (confidence interval) and their rate gradually decrease in amplitude down to the depth of –11 m below the ground surface. Lack of their oscillations below the depth of –11 m shows data homogeneity in this region that could be associated with homogenous character of soil in this region and hence the absence of soil contamination there. That is why values of ''wet zone'' below the depth of –11 m could be related with ''background values''—values caused by saturated clays or wet salted clayey sands. Figure 3 shows that such background value is similar to 0.25 million m^3. Note the existence of small

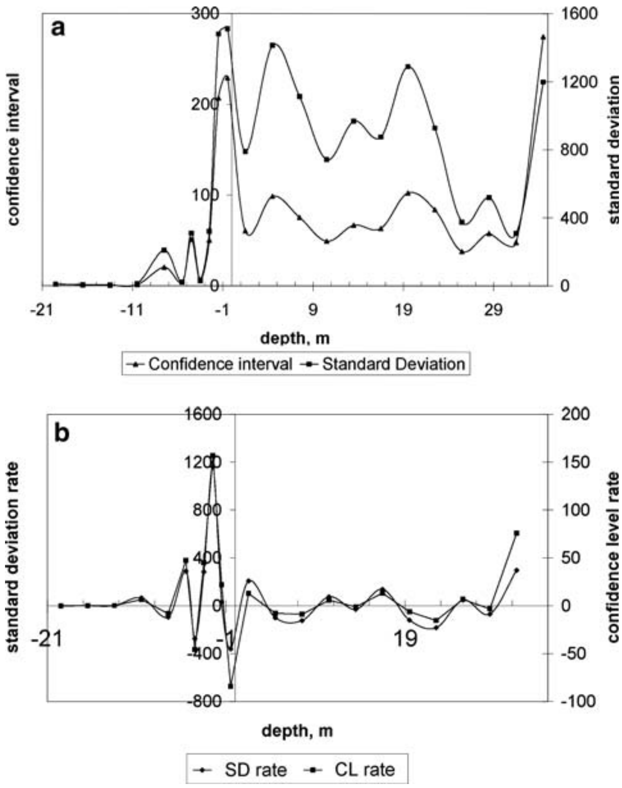

Fig. 4 **a** Changes of standard deviation and confidence interval versus depth of the waste body. **b** Changes of standard deviation rate and confidence interval rate versus depth of the waste body

''jump'' of ''wet zone'' value (0.35 million m^3) at the depth of –7 m below the ground surface. Taking background value (0.25) away from this value (0.35) yields the ''wet zone'' value at this depth to be 0.05 million m^3 implying a decrease in estimated volume of soil contamination by factor 50: from 1 million m^3 down to 0.2 million m^3.

As we noted above, two lithological facies of clays interbedded with clayey sand underlay the bottom boundary of the waste disposal. Permeability coefficient of fat clays in this region is of the order of 10^{-8} cm/s, while one of clayey sand has 10^{-4} to 10^{-5} cm/s (Liskevich et al. 2003). Hence, contaminant penetration through the bottom boundary of the waste disposal could be associated with the existence of clayey sand lenses there.

Conclusions

Electrical resistivity imaging is a commercially available method intensively applied for characterization of natural and artificial materials in different geo-engineering situations. Its application to waste disposal investigations, where lechates accumulated inside a waste body are an extreme environmental hazard, frequently allows not only a continuous study into a waste disposal but also a significant cost reduction as compared to conventional drilling method. However, in the special case that electrical resistivity of underlying soil is similar to that of leachate, accurate observation of the boundary between waste disposal and soil presents a challenge. Our investigation has shown that application of simple statistical procedure allows us to determine this boundary accurately on the basis of changes of standard deviation (and confidence interval). Differences in standard deviation (and confidence interval) result from different geneses of artificial (waste disposal) and natural (underlying soil) objects.

Moreover, our approach enables us to estimate the volume of contaminant penetration into the soil under the bottom boundary of waste disposal and hence more accurately assess the impact of the waste disposal on environment in the region.

References

Abu-Zeid N, Santarato G (2004) On the correspondence between resistivity and texture of loose sediments, saturated with salt water. Near Surf Geophys 3:144–149

Abu-Zeid N, Bianchini G, Santarato G, Vaccaro C (2004) Geochemical characterization and geophysical mapping of Landfill leachates: the Marozzo canal case study (NE Italy). Environ Geol 45:439–447

Aristodemou E, Thomas-Betts A (2000) DC resistivity and induced polarisation investigations at a waste disposal site and its environments. J Appl Geophys 44:275–302

Batayneh AT, Barjous MO (2004) Resistivity surveys near a waste-disposal site in the Qasr Tuba area of central Jordan. Bull Eng Geol Environ 64(3):285–291

Bernstone C, Dahlin T, Ohlsson T, Hogland W (2000) DC-resistivity mapping of internal landfill structures: two pre-excavation surveys. Environ Geol 39(3–4):360–368

Bowling JC, Rodriguez AB, Harry DL, Zheng C (2005) Delineating alluvial aquifer heterogeneity using resistivity and GPR data. Ground Water 43(6):890–903

Cardarelli E, Bernabini M, (1997) Two case studies of the determination of parameters of urban waste dumps. J Appl Geophys 36:167–174

Cardarelli E, Fischanger F (2006) 2D data modelling by electrical resistivity tomography for complex subsurface geology. Geophys Prospect 54:121–133

Chandra S, Rao VA, Krishnamurthy NS, Dutta S, Ahmed S (2006) Integrated studies for characterization of lineaments used to locate groundwater potential zones in a hard rock region of Karnataka, India. Hydrogeol J 14:767–776

Dahlin T (2001) The development of DC resistivity imaging techniques. Comput Geosci 27:1019–1029

Dahlin T, Loke MH (1998) Resolution of 2D Wenner resistivity imaging as assessed by numerical modelling. J Appl Geophys 38:237–249

Dahlin T, Zhou B (2002) Gradient and mid-point-referred measurements for multi-channel 2D resistivity imaging. In: Proceedings of the 8th meeting environmental and engineering geophysics, Aveiro, Portugal 8–12 September 2002, pp 157–161

Dahlin T, Zhou B (2004) A numerical comparison of 2D resistivity imaging with 10 electrode arrays. Geophys Prospect 52:379–398
De Domenico D, Giannino F, LeucciG, Bottari C (2006) Integrated geophysical surveys at the archaeological site of Tindari (Sicily, Italy). J Archaeol Sci 33:961–970
Depountis N, Harris C, Davies MCR, Koukis G, Sabatakakis N (2005) Application of electrical imaging to leachate plume evolution studies under in-situ and model conditions. Environ Geol 47:907–914
Dogan M, Papamarinopoulos S (2006) Exploration of the Hellenistic fortification complex at Asea using a multigeophysical prospection approach. Archaeol Prospect 13:1–9
Drahor MG, Gokturkler G, Berge MA, Kurtulmus TO (2006) Application of electrical resistivity tomography technique for investigation of landslides: a case from Turkey. Environ Geol 50:147–155
Froese DG, Smith DG, Clement DT (2005) Characterizing large river history with shallow geophysics: Middle Yukon River, Yukon Territory and Alaska. Geomorphology 67:391–406
Gawande NA, Reinhart DR, Thomas PA, McCreanor PT, Townsend TG (2003) Municipal solid waste in situ moisture content measurement using an electrical resistance sensor. Waste Management 23:667–674
Gibert D, Nicollin F, Kergosien B, Bossart P, Nussbaum C, Grislin-Mouëzy A, Conil F, Hoteit N (2006) Electrical tomography monitoring of the excavation damaged zone of the Gallery 04 in the Mont Terri rock laboratory: Field experiments, modelling, and relationship with structural geology. Appl Clay Sci 33:21–34
Godio A, Strobbia C, De Bacco G 2006 Geophysical characterization of a rockslide in an alpine region. Eng Geol 83:273– 286
Grandjean G, Pennetier C, Bitri A, Meric O, Malet J-P (2006) Caractérisation de la structure interne et de l'état hydrique de glissements argilo-marneux par tomographie géophysique: l'exemple du glissement-coulée de Super-Sauze (Alpes du Sud, France). C R Geosci 338:587–595
Guerin R, Munoz ML, Christophe A, Laperrelle C, Hidra M, Drouart E, Grellier S (2004) Leachate recirculation: moisture content assessment by means of a geophysical technique. Waste Manag 24:785–794
Gurion I, Novik A (2003) Reconstruction of Har AEshpa (Haifa). Report number 1
Hack R (2000) Geophysics for slope stability. Surv Geophys 21:423–448
Hamzah U, Yaacup R, Samsudin A, Ayub MS 2006 Electrical imaging of the groundwater aquifer at Banting, Selangor, Malaysia. Environ Geol 49:1156–1162
Hunt P, Powell N, Watson KA (2001) Limiting apparent-resistivity values for dipping-bed earth models. Geophys Prospect 49:577–591
Khesin B (2005) Use of geophysical methods for the solution of environmental problems in Israel. HAIT J Sci Eng 2(1–2):95–124
Khesin B, Alexeyev V, Eppelbaum L (1996) Interpretation of geophysical fields in complicated environments bookseries. Modern approaches in geophysics, vol 14. Kluwer, Dordrecht
Kneisel C (2006) Assessment of subsurface lithology in mountain environments using 2D resistivity imaging. Geomorphology 80:32–44
Leucci G (2006) Contribution of Ground Penetrating Radar and Electrical Resistivity Tomography to identify the cavity and fractures under the main Church in Botrugno (Lecce, Italy). J Archaeol Sci 33:1194–1204
Liskevich D, Shulov S, Doudkinski D, Roslik A (2003) Physical and mechanical properties of the soft soils of the Kishon River's delta and flood lands. In: Proceedings of the international geotechnical symposium: foundation engineering on problematic soil ground, St. Petersburg, pp 164–167
Loke MH (2000) Electrical imaging surveys for environmental and engineering studies. A practical guide to 2-D and 3-D surveys, p 61. http://www.heritagegeophysicscom/images/lokenotepdf
Loke MH, Barker RD (1995) Improvements to the Zohby method for the inversion of resistivity sounding and pseudosection data. Comput Geosci 21(2):321–332
Loke MH, Barker RD (1996a) Practical techniques for 3D resistivity surveys and data inversion. Geophys Prospect 44:499–523
Loke MH, Barker RD (1996b) Rapid least squares inversion of apparent resistivity pseudosections by a quasi- Newton method. Geophys Prospect 44:131–152
Loke MH, Dahlin T (2002) A comparison of the Gauss–Newton and quasi-Newton methods in resistivity imaging inversion. J Appl Geophys 49:149–162
Martinho E, Almeida F (2006) 3D behaviour of contamination in landfill sites using 2D resistivity/IP imaging: case studies in Portugal. Environ Geol 49:1071–1078
Nassir SS, Loke MH, Lee CY, Nawawi MNM (2000) Salt-water intrusion mapping by geoelectrical imaging surveys. Geophys Prospect 48:647–661
Nguyen F, Garambois S, Jongmans D, Pirard E, Loke MH (2005) Image processing of 2D resistivity data for imaging faults. J Appl Geophys 57:260–277
Panissod C, Michot D, Benderitter Y, Tabbagh A (2001) On the effectiveness of 2D electrical inversion results: an agricultural case study. Geophys Prospect 49:570–576
Porsani JL, Elis VR, Hiodo FY (2005) Geophysical investigations for the characterization of fractured rock aquifers in Itu, SE Brazil. J Appl Geophys 57:119–128
Reccelli-Snyder H L, Stahl B, Leberfinger A, Warren PG, Warren JJ (1997) Electrical imaging: A Method for Identifying Potential Collapse and other Karst Features Near Roadways. Science Applications International Corporation, Middletown, Pennsylvania. http://www.quality-geophysicscom/50th1pdf
Rey E, Jongmans D, Gotteland P, Garambois S (2006) Characterisation of soils with stony inclusions using geoelectrical measurements. J Appl Geophys 58:188–201
Rizzo E, Colella A, Lapenna V, Piscitelli S (2004) High-resolution images of the fault-controlled High Agri Valley basin (Southern Italy) with deep and shallow electrical resistivity tomographies. Phys Chem Earth 29:321–327
Sharma PV (1997) Environmental and engineering geophysics. Cambridge University Press, Cambridge
Sherif M, El Mahmoudi A, Garamoon H, Kacimov A, Akram S, Ebraheem A, Shetty A (2006) Geoelectrical and hydrogeochemical studies for delineating seawater intrusion in the outlet of Wadi Ham, UAE. Environ Geol 49:536–551
Storz H, Storz W, Jacobs F (2000) Electrical resistivity tomography to investigate geological structures of the earth's upper crust. Geophys Prospect 48:455–471
Takahashi T (2004) ISRM Suggested Methods for land geophysics in rock engineering. Int J Rock Mech Mining Sci 41:885–914
Takahashi T, Takeuchi T, Sassa K (2006) ISRM Suggested Methods for borehole geophysics in rock engineering. Int J Rock Mech Mining Sci 43:337–368
Vafidis A, Economou N, Ganiatsos Y, Manakou M, Poulioudis G, Sourlas G, Vrontaki E, Sarris A, Guy M, Kalpaxis Th (2005) Integrated geophysical studies at ancient Itanos (Greece). J Archaeol Sci 32:1023–1036
Wu X, Yifei X, Qi C, Wang T (2003) Computations of secondary potential for 3D DC resistivity modeling using an incomplete Choleski conjugate-gradient method. Geophys Prospect 51:5678–577
Zume JT, Tarhule A, Christenson S (2006) Subsurface imaging of an abandoned solid waste landfill site in Norman, Oklahoma. Ground Water Monit Remediat 26(2):62–69